Contribution from LURE,[1] Université de Paris-Sud, 91405 Orsay, France, the Laboratoire de Physicochimie Structurale, Université de Paris-Val de Marne, 94000 Créteil, France, the Laboratoire de Chimie Théorique, ERA No. 22, Université de Nancy I, Nancy, France, and the Laboratoire de Spectrochimie des Elêments de Transition, ERA No. 672, Université de Paris-Sud, 91405 Orsay, France

EXAFS Determination of the Copper Oxalate Structure. Relation between Structure and Magnetic Properties

A. MICHALOWICZ,*[2a] J. J. GIRERD,[2b] and J. GOULON[2c]

Received February 20, 1979

The structure of copper oxalate($Cu^{II}C_2O_4 \cdot {}^1/_3H_2O$) is studied by extended X-ray absorption fine structure spectroscopy. Two structures were previously proposed: one similar to the iron oxalate chain ($FeC_2O_4 \cdot 2H_2O$) or one close to the copper acetate coordination site. The main difference between these two models is the value of the first metal–metal distance: greater than 5 Å in the first case and less than 3 Å in the second case. The comparative study of X-ray absorption spectra of $CuC_2O_4 \cdot {}^1/_3H_2O$ and of compounds of known structure, either with a long or with a short first metal–metal distance, indicates clearly that the second shell surrounding a Cu(II) ion is exclusively composed of light atoms. For the first shell, the four Cu–O distances are within 1.98 ± 0.02 Å. These results are consistent with the first model and do not agree with the second one. The knowledge of this structure is essential to include $Cu^{II}C_2O_4 \cdot {}^1/_3H_2O$ in the discussion of the magnetic exchange in Cu(II) binuclear and chain compounds with oxalate ions as bridging ligands. The published values of J for such compounds indicate that (i) an important antiferromagnetic coupling does not involve necessarily a short metal–metal distance (for instance, $J = -272$ cm^{-1} for $CuC_2O_4 \cdot {}^1/_3H_2O$) and (ii) the intensity of this exchange is very sensitive to the symmetry of the Cu(II) site ($J = 0$ for $Cu_2C_2O_4(dien)_2(ClO_4)_2$). These facts are explained by the preponderance of the σ-type $d_{x^2-y^2}$ pathway for the magnetic exchange.

Introduction

The magnetic properties of copper oxalate ($CuC_2O_4 \cdot {}^1/_3H_2O$) are well-known.[3,4] They are the result of a long chain of equivalent and equidistant Cu(II) ions and have been interpreted with the 1-D Heisenberg Hamiltonian[5,6] $-J \times \sum_{a=0}^{N-1} S_a \cdot S_{a+1}$, $S_N = S_0$, $N \rightarrow \infty$. The determined exchange parameter is $J = -272$ cm^{-1}.

According to these magnetic properties, two structural models have been proposed (Figure 1) by Dubicki et al. So far, all attempts to grow single crystals have been unsuccessful. The first model (Figure 1) was found in $Cu(NH_3)_2C_2O_4 \cdot 2H_2O$[7] and $FeC_2O_4 \cdot 2H_2O$.[8a] In the second model, the coordination of the oxalate ion is similar to that found in $Cu(CO_2(CH_2)_2CO_2) \cdot 2H_2O$[4] and copper acetate binuclear compounds.[10] An important structural difference between these two models is the first metal–metal distance (5.56 Å in $FeC_2O_4 \cdot 2H_2O$ and 2.61 Å in $Cu(CO_2(CH_2)_2CO_2) \cdot 2H_2O$). A previous argument in favor of the second model was the value of the exchange parameter, similar to those of the copper acetate type complexes. The EPR study of $CuC_2O_4 \cdot {}^1/_3H_2O$[5] confirmed the long chain structure but was unable to eliminate conclusively either of the two models. In order to understand the importance of the exchange parameter in this compound, we believe knowledge of the structure is of the utmost importance.

$CuC_2O_4 \cdot {}^1/_3H_2O$ is obtained as a microcrystalline powder and gives a Debye–Scherrer pattern. Instead of trying to solve the structure from this powder pattern,[8b] we have decided to use a novel technique, extended X-ray absorption fine structure (EXAFS). Information is derived from the oscillatory component of the X-ray absorption spectrum on the high-energy side of an X-ray absorption edge (the K edge of copper in our case). This technique does not require single crystals and the structural data obtained are essentially the distances—not the angles—between a specific central atom and its neighbors. A major effort toward developing EXAFS is being made in the synchrotron radiation centers. Storage rings or synchrotrons are the most powerful tunable sources of X-rays conveniently suitable for X-ray absorption spectroscopy.[11-19]

Experimental and Data Analysis Section

This structural study is carried out by comparison of the spectra of the compound of unknown structure ($CuC_2O_4 \cdot {}^1/_3H_2O$) and of structurally known model compounds. We have chosen two compounds with a short copper–copper distance, copper acetate–pyrazine[10] ($Cu_2(CH_3CO_2)_4pyz$) and bis(bipyridyl)dihydroxodicopper nitrate[23] ($Cu_2(OH)_2(bpy)_2(NO_3)_2$), and also $FeC_2O_4 \cdot 2H_2O$, which is characterized by its long metal–metal distance and is practically isomorphous to the first proposed model. $CuC_2O_4 \cdot {}^1/_3H_2O$ was synthesized as in ref 4, $FeC_2O_4 \cdot 2H_2O$ was obtained in a similar way, and $Cu_2(CH_3CO_2)_4pyz$ was synthesized as in ref 10.

The spectra of these compounds have been recorded at LURE,[24] the French synchrotron radiation facility, by using the X-rays emitted by the ultrarelativistic electron beam of the storage ring DCI, with the following parameters: electron energy = 1.72 GeV, average current = 130 mA. The experimental setup is completely described elsewhere.[15,16] The samples are parallelepipedic pellets (40 × 5 × 0.1 mm). Each spectrum is in fact the sum of three independent recordings added after individual inspection. All the spectra are recorded at room temperature.

An X-ray absorption spectrum ($\ln (I_0/I)$ vs. the photon energy $h\nu$) presents three regions (Figure 2): (i) a smooth preedge decay, (ii) the edge corresponding to the ejection of a deep level electron of the specific atom (a 1s electron of copper in our case), (iii) the superposition of a background and the EXAFS oscillations from 50 to 700 eV above the edge.

The first step of the analysis is a pre- and postedge background removal, an arbitrary choice of the energy threshold E_0[38] (above which the photoelectron is considered as free), and a transformation from the photon energy $h\nu$ to the photoelectron wave vector $k = [(2me/\hbar^2)(h\nu - E_0)]^{1/2}$. The next steps are derived from the standard EXAFS formula obtained by the theory.[20-22]

$$\chi(k) = \frac{1}{k}\sum_i \frac{|f_i(k)|N_i}{R_i^2} \sin(2kR_i + \alpha_i(k)) e^{-2\sigma_i^2 k^2} e^{-2R_i/\lambda} \qquad (1)$$

with $\chi(k) = (\mu - \mu_0)/\mu_0$ the normalized oscillatory component of the absorption coefficient, R_i the central atom–neighbor distance, N_i the number of equivalent atoms in a shell, $f_i(k)$ and $\alpha_i(k)$ the amplitude and phase-shift functions characteristic of the ejection of an electron from the central atom and its back-scattering by the neighbors, σ_i a damping coefficient due to thermal vibration and distance distortions of the shell, and λ the mean free path of the photoelectron. The sum includes all the shells of atoms surrounding the absorber. This formula is valid for $k \geq 4$ Å^{-1} and assumes that each absorber–neighbor pair is independent. Mutual shadowing of outer shells and multiple scattering of the photoelectron are not considered. In practice, these effects may affect the amplitude and phase shifts and give extra components in the spectra.

The spectra analysis includes the following. (i) There is Fourier transformation of $k^3(\chi(k))$ from k to R space, where each shell is represented by a peak. (ii) Simulation of the R-space spectra is done by using formula 1, when the structure is known or assumed. For these simulations, we use the amplitude and phase shift functions

0020-1669/79/1318-3004$01.00/0

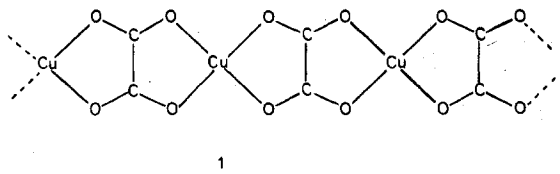

1

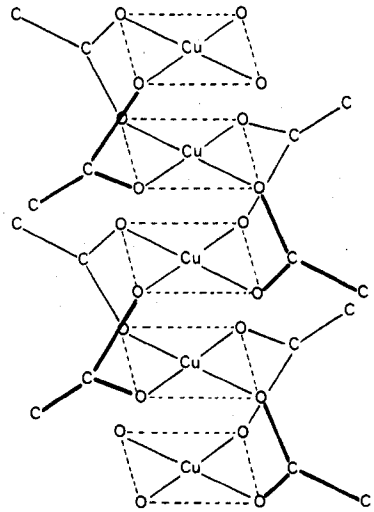

2

Figure 1. (1) Possible structure for $CuC_2O_4 \cdot {}^1/_3H_2O$ involving the Cu_n chain. (2) Alternative structure for $CuC_2O_4 \cdot {}^1/_3H_2O$.

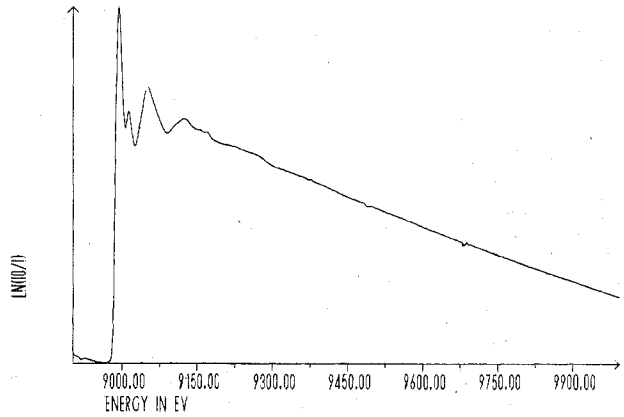

Figure 2. X-ray absorption spectrum of $CuC_2O_4 \cdot {}^1/_3H_2O$.

parameterized and tabulated for a great number of absorber–neighbor pairs by Lee and Teo.[22]

$$f_i(k) = A_i/(1 + B_i^2(C_i - k)^2)$$
$$\alpha_i(k) = a_i + b_ik + c_ik^2 + d_i/k^3 \qquad (2)$$

Average values of λ (8 Å) and $2\sigma^2$ (0.01 Å^2) are used since, compared to the experimental spectra, they lead to reasonable amplitudes and widths of the peaks for all our model compounds. (iii) A Fourier filtered spectrum in the k space by an inverse Fourier transformation of this peak is obtained when a peak is well resolved and assigned to a single shell and when adequate windows are used.

The radius of the shell is then obtained by a least-squares fitting to the simplified expression

$$\chi(k) = A\frac{f(k)}{k} \sin (2kR + \alpha(k))e^{-2\sigma^2k^2} \qquad (3)$$

A is a linear scaling parameter and the nonlinear fitted parameters are R, σ, and E_0. The quality of the fit is determined by a residual factor

$$\rho = \sum_k(\chi_{exptl} - \chi_{calcd})^2/\sum_k\chi_{exptl}^2$$

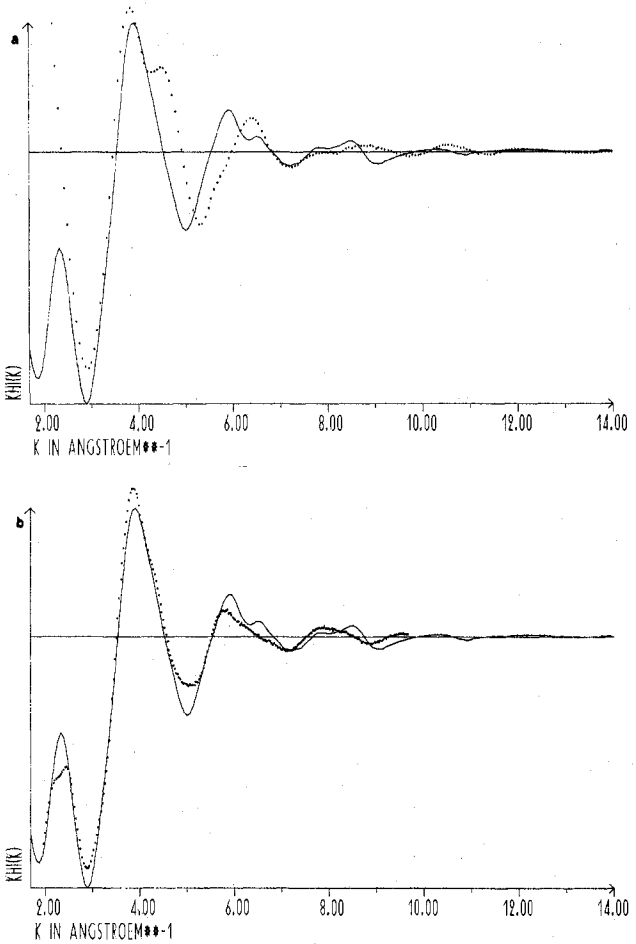

Figure 3. $\chi(k)$ spectra of $CuC_2O_4 \cdot {}^1/_3H_2O$ and $Cu_2(CH_3CO_2)_4pyz$ (a) and $CuC_2O_4 \cdot {}^1/_3H_2O$ and $FeC_2O_4 \cdot 2H_2O$ (b). The energy threshold E_0 is chosen on the maximum of the absorption edge: 3995 eV for the copper compound and 7120 eV for $FeC_2O_4 \cdot 2H_2O$. (In all the EXAFS figures of this work vertical units are arbitrary.)

Table I. Nature of the Second Shell and Amplitude of the Corresponding Peak Relative to the One of the First Shell Peak (See Text) for the Compounds Studied

compd	nature of the 2nd shell	rel amplitude	fig
$Cu_2(CH_3CO_2)_4pyz$	1 copper at 2.58 Å	0.51	5a
$Cu_2(OH)_2(bpy)_2(NO_3)_2$	1 copper at 2.84 Å	0.63	5b
$Fe(C_2O_4) \cdot 2H_2O$	4 carbons at 2.89 Å	0.27	5d
$CuC_2O_4 \cdot {}^1/_2H_2O$	?	0.27	5c

The accuracy of this distance determination depends on the use of the tabulated phase shifts[22] as universal, regardless of the nature of the bonding. This transferability of phase shifts has been tested for a great number of model compounds[11-22] and the discrepancy between known and EXAFS distances was always found to be less than 0.02 Å for the first shell.

Results

The EXAFS of $CuC_2O_4 \cdot {}^1/_3H_2O$ and of two model compounds are superposed in Figure 3. The coincidence is rapidly lost in Figure 3a while in Figure 3b the spectra are more similar with a slight difference in frequency.

The real part and amplitude of the Fourier transform spectra are represented in Figure 4. Since our choice between the two models will be determined by the value of the first Cu–Cu distance, we must analyze the effect of such a metal–metal shell at a short distance ($R < 3$ Å). Table I gives the experimental relative amplitudes of the second peak compared to the metal–light atom first shell. Experimentally, a short

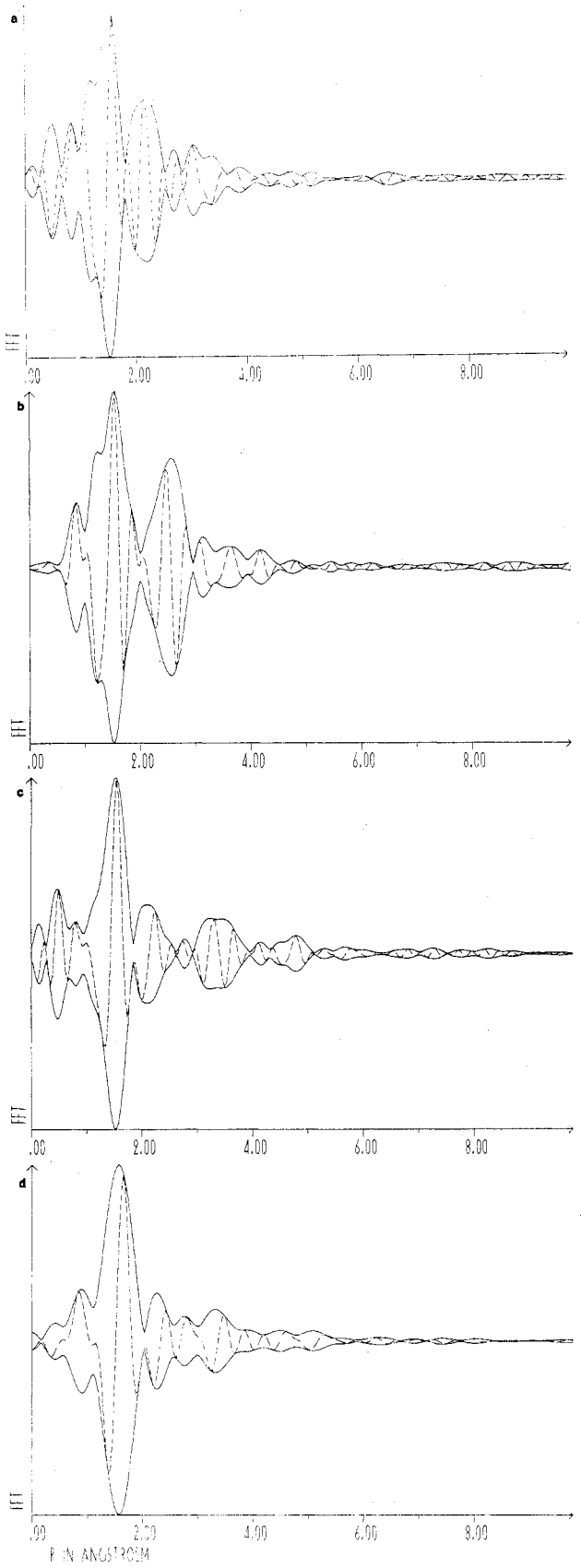

Figure 4. Experimental *R*-space spectra of two short distance Cu–Cu model compounds (a and b), one long metal–metal distance model compound, and $CuC_2O_4 \cdot {}^1/_3H_2O$. These spectra are obtained by a Fourier transformation of the *k*-space EXAFS spectra $\chi(k)$ weighted by a factor k^3. Real part (---) and modulus (—) for (a) $Cu_2(CH_3CO_2)_4pyz$, (b) $Cu_2(OH)_2(bpy)_2(NO_3)_2$, (c) $CuC_2O_4 \cdot {}^1/_3H_2O$, and (d) $FeC_2O_4 \cdot 2H_2O$.

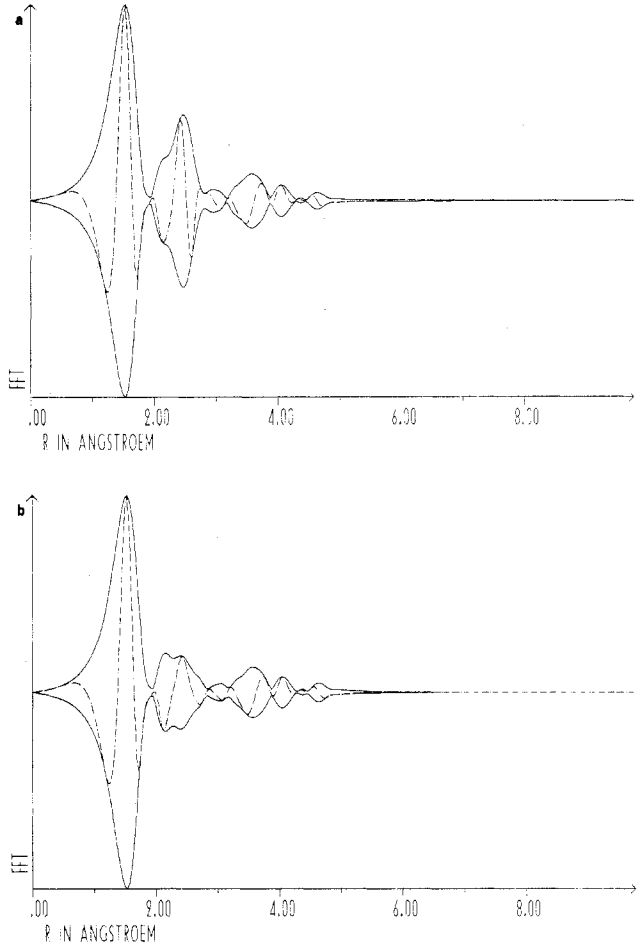

Figure 5. Simulated *R*-space spectrum of a short distance Cu–Cu model compound using the distances determined by X-ray crystallography and the standard formula for $\chi(k)$ (a). In part b the Cu–Cu shell is ignored in order to show its relative importance in the spectrum.

Cu–Cu distance gives a peak approximately twice as intense as the one for four light atoms, shifted by about −0.4 Å from its actual *R* value. This amplitude effect may be reproduced on simulated spectra, for instance, for the dihydroxo-bridged copper dimer (Figure 5a). When we ignore the Cu–Cu shell in the simulation, the spectrum of Figure 5a is reduced to that of Figure 5b with a weak second peak due to light atoms present at this distance. The agreement between theory and data is good for the first two shells but poorer for $R > 3$ Å. This is due to the experimental noise, the effects of shadowing, and the multiple scattering mentioned previously.

In the *R*-space spectrum of $CuC_2O_4 \cdot {}^1/_3H_2O$ (Figure 4c) the second peak is twice as small as expected for a shell of *one* copper (in the second model, this shell should be composed of *two* coppers). Thus this peak is probably representative of a light atom shell.

The filtering and fitting procedures are used on the first two shells of the copper compounds. The results are given in Table II and on Figure 6. Comments on the results are as follows. (i) The determined Cu–Cu distances in the binuclear compounds are in very good agreement with the crystallographic data. (ii) The same remark holds for the first Cu–O shell of $Cu_2(CH_3CO_2)_4pyz$. (This gives good confidence for our determination of the average Cu–O distance in $CuC_2O_4 \cdot {}^1/_3H_2O$ of $R_{Cu-O} = 1.98 \pm 0.02$ Å. A qualitative discussion of the actual values of each Cu–O distance in $CuC_2O_4 \cdot {}^1/_3H_2O$ is possible by comparing the damping coefficients found for $Cu_2(CH_3CO_2)_4pyz$ ($2\sigma^2 = 0.021$ Å^2 and $\Delta R = 0.004$ Å) and $CuC_2O_4 \cdot {}^1/_3H_2O$ ($2\sigma^2 = 0.017$ Å^2). On the assumption that the thermal vibrations are similar in both compounds, the four

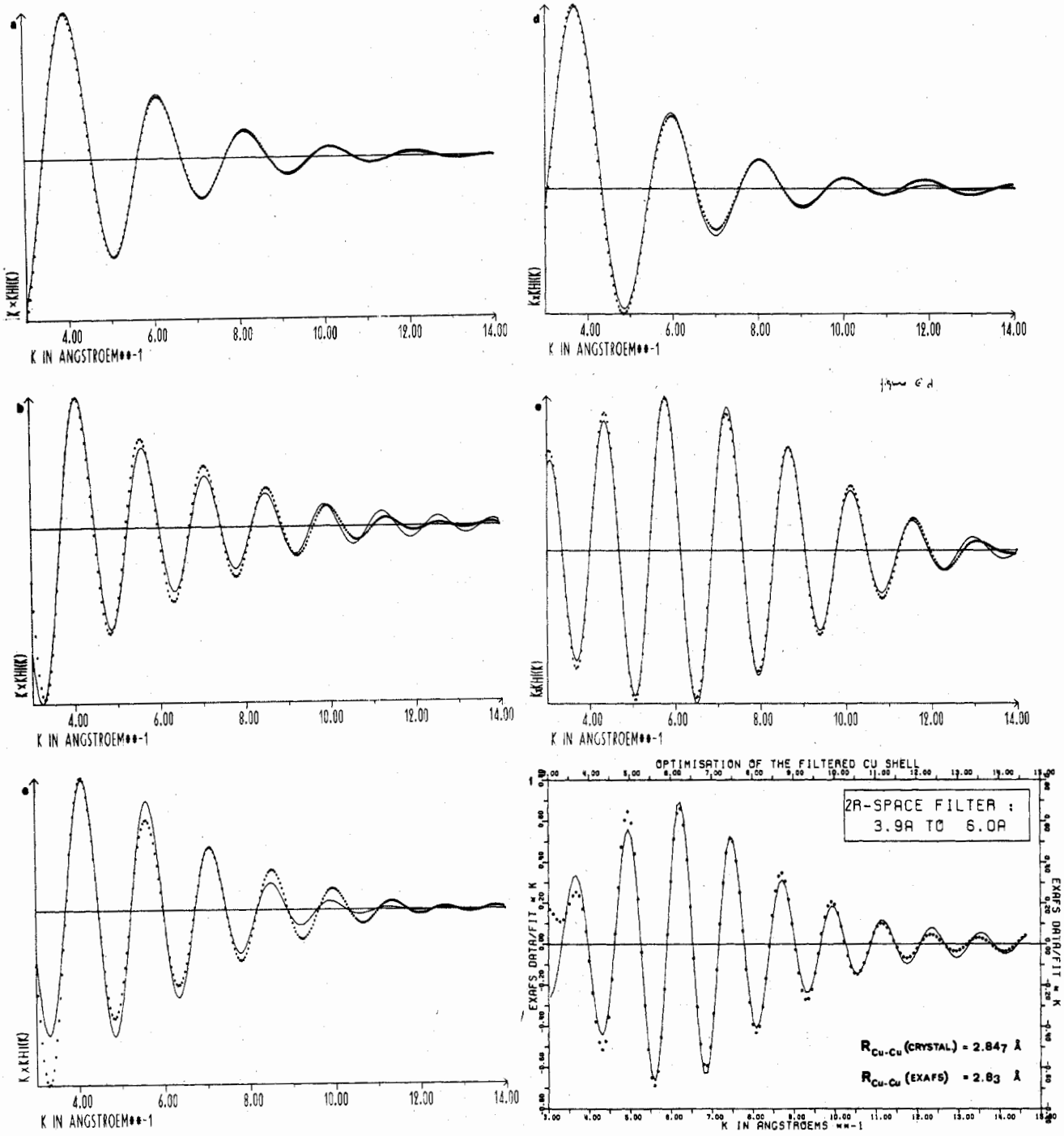

Figure 6. Least-squares fitting (—) of the filtered experimental data (···): (a) Cu–O shell of $CuC_2O_4 \cdot {}^1/_3H_2O$, (b) Cu–Cu shell of $CuC_2O_4 \cdot {}^1/_3H_2O$, (c) the second shell of $CuC_2O_4 \cdot {}^1/_3H_2O$ considered as a Cu–Cu shell (the best fit obtained), (d) Cu–O shell of $Cu_2(CH_3CO_2)_4pyz$, (e) Cu–Cu shell of $Cu_2(CH_3CO_2)_4pyz$, (f) Cu–Cu shell of $Cu_2(OH)_2(bpy)_2(NO_3)_2$.

Table II. Fitting Results of the First Two Shells of Copper Compounds

	shell	E_0, eV	R_{EXAFS}, Å	R_{cryst}, Å	$2\sigma^2$, Å^2	ρ, %	fig
$CuC_2O_4 \cdot {}^1/_3H_2O$	1st Cu–O	8990	1.98		0.017	1	7a
	2nd Cu–C	8992	2.65		0.010	3	7b
	2nd Cu–Cu	8988[a]	2.46		0.045	11	
	2nd Cu–Cu	8967	2.66		0.043	6	7c
$Cu_2(CH_3CO_2)_4pyz$	1st Cu–O	8991	1.96	1.964	0.021	1.2	7d
	2nd Cu–Cu	8988	2.58	2.583	0.005	0.4	7e
$Cu_2(OH)_2(byp)_2(NO_3)_2$	2nd Cu–Cu	8993[a]	2.83	2.847			7f

[a] Fixed values.

Cu–O distances are within 1.98 ± 0.02 Å.) (iii) The characterization of the second shell of $CuC_2O_4 \cdot {}^1/_3H_2O$ may be completed by the shape of the amplitude of $k(\chi(k))$ which exhibits a peak at $k = 6$ Å^{-1} for the Cu–Cu shells (Figure 6e,f) and probably for $k < 3$ Å^{-1} in the light atom shells (Figure 6a,d).

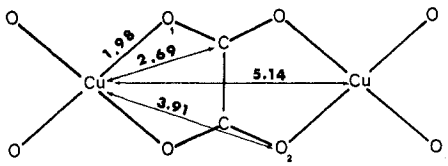

Figure 7. Determined distances for $CuC_2O_4 \cdot {}^1/_3H_2O$: Cu–O by EXAFS; Cu–C by EXAFS (2.65 Å) and by geometry (2.69 Å); the others by geometry.

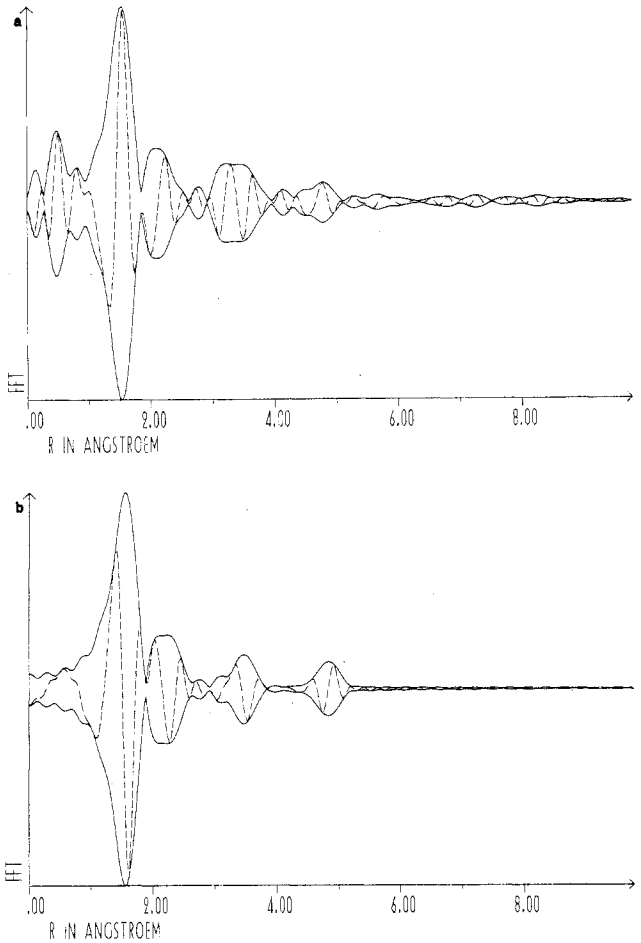

Figure 8. Comparison of experimental (a) and theoretical (b) *R*-space spectra for $CuC_2O_4 \cdot {}^1/_3H_2O$.

Thus any attempt to fit the second shell of $CuC_2O_4 \cdot {}^1/_3H_2O$ leads to bad residual factors and (or) a doubtful value of E_0. On the other hand, a satisfying fit is obtained for a Cu–C shell with $R_{Cu-C} = 2.65$ Å. With the determination of the first shell radius and the assumption of the same geometry for the oxalate ion in $FeC_2O_4 \cdot 2H_2O$ and $CuC_2O_4 \cdot {}^1/_3H_2O$, it is possible to compute all the copper–neighbor distances and compare the experimental and simulated spectra. For the first model (Figure 7) we obtain $R_{Cu-O(1)} = 1.98$ Å, $R_{Cu-C} = 2.69$ Å, $R_{Cu-O(2)} = 3.91$ Å, and $R_{Cu-Cu} = 5.14$ Å. With these values the agreement between theoretical and experimental *R*-space spectra (Figure 8) is fairly good. Moreover, the Cu–C distance determined by EXAFS (2.65 Å) is close to the geometrically determined value (2.69 Å).

The results obtained in the first two shells $R_{Cu-O} = 1.98$ Å and $R_{Cu-C} \simeq 2.7$ Å, damping coefficients consistent with a rather rigid chain, and no visible Cu–Cu shell in the range 2.5–3.5 Å are incompatible with the second model. For the same reason a planar layer model must be ruled out.

Two structural problems are not solved by this EXAFS analysis: (i) What about an interaction between adjacent ribbons? Since a reliable assignment of a Cu–Cu shell is impossible with this room-temperature spectrum, the question is still open. (ii) The Cu(II) site could be tetrahedral with the oxalate ions twisted 90°. However it should be observed that: to the best of our knowledge, there is no example of a tetrahedral structure for the $Cu^{II}O_4$ chromophore; addition of ammonia to $CuC_2O_4 \cdot {}^1/_3H_2O$ leads to $CuC_2O_4(NH_3)_2 \cdot 2H_2O$ which has a trans ribbon structure; 1:2 complexes of Cu(II) with oxalate anion are planar;[39] and the Cu(II) chain with 90° twisted oxalate would lead to orthogonal magnetic orbitals and hence to a ferromagnetic coupling.[40]

Owing to our EXAFS analysis and the points mentioned above, we propose a ribbon structure with a square-planar coordination of Cu(II) for $CuC_2O_4 \cdot {}^1/_3H_2O$.

Table III. Structure and Exchange Parameter for Some Oxalato-Bridged Complexes

compd	$-J$, cm^{-1}	ref	structure	ref
$CuC_2O_4 \cdot {}^1/_2H_2O$	272	5	chain	this work
$NiC_2O_4(2MIz)_2$[a]	24	9	chain	9
$CoC_2O_4(2MIz)_2$[a]	19[b]	9	chain	9
$FeC_2O_4 \cdot 2H_2O$	6.8	28	chain[c]	8
$CuC_2O_4 \cdot NH_3$	266	29	binuclear[c]	29
$Cu_2C_2O_4(Et_5dien)_2(BPh_4)_2$	74.8	25	binuclear[c]	25
$Cu_2C_2O_4(dien)_2(ClO_4)_2$	0	25	binuclear[c]	30
$Cu_2C_2S_2(NCH_2CH_2OH)_2 \cdot 2H_2O \cdot SO_4$	594	31	binuclear[c]	31

[a] 2MIz = 2-methylimidazole. [b] Ising model was used. [c] X-ray determined structure.

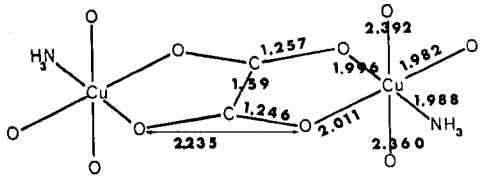

Figure 9. Structure of $CuC_2O_4NH_3$ as determined by Cavalca et al.[29]

Discussion of the Magnetic Properties

It is now established that for the same transition ions and bridging ligands, drastic variation of the exchange parameter occurs with slight modifications of the structure due to terminal ligands and counteranions.[25-27] The study of systems where the ligand oxalate is bridging two transition ions in binuclear molecules and chains is well developed. The results which have been published concerning such systems are summarized in Table III. A $[Cu_2C_2S_2(NCH_2CH_2OH)_2 \cdot 2H_2O]^{2+}$ ion studied in our laboratory[1b,31] where the Cu(II) ion has the same coordination is included (Figure 11).

The exchange parameter was obtained for the chains by the Heisenberg unidimensional Hamiltonian $-J\sum_a S_a \cdot S_{a+1}$ and for the binuclear complex by the Heisenberg Hamiltonian $-JS_1 \cdot S_2$. It has been shown[32] that for a linear chain and for a binuclear system with the same metal-bridging ligand–metal network, the exchange parameters have to be essentially the same. An example[35] of this is given by the chain $N(CH_3)_4MnCl_3$ ($J = -8.8$ cm^{-1})[33] and the binuclear $Mn_2Cl_9^{5-}$ ($J = -8.6$ cm^{-1}).[34] The comparison of $CuC_2O_4 \cdot {}^1/_3H_2O$ and $CuC_2O_4 \cdot NH_3$ is in fact another example of this same property. The exchange parameters of these two compounds are very close (−272 and −266 cm^{-1}). This is also true of their structures (Figures 7 and 9). The shortest copper-coordinated atom distances are in the plane of the oxalate ligand. The Cu(II) unpaired electron is therefore in the $d_{x^2-y^2}$ orbital, pointing toward the oxygen bridging atoms. In Cu(II) binuclear molecules the energy splitting between the two last molecular orbitals occupied in the triplet state is responsible for the antiferromagnetic coupling.[32,36,37] These orbitals are represented in Figure 10[31] for the binuclear compound. They are similar in

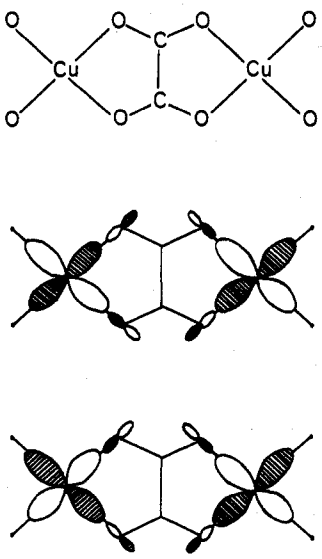

Figure 10. Schematic representation of the molecular orbitals singly occupied in the triplet state of a dimeric fragment of the linear chain $CuC_2O_4 \cdot {}^1/_3H_2O$.

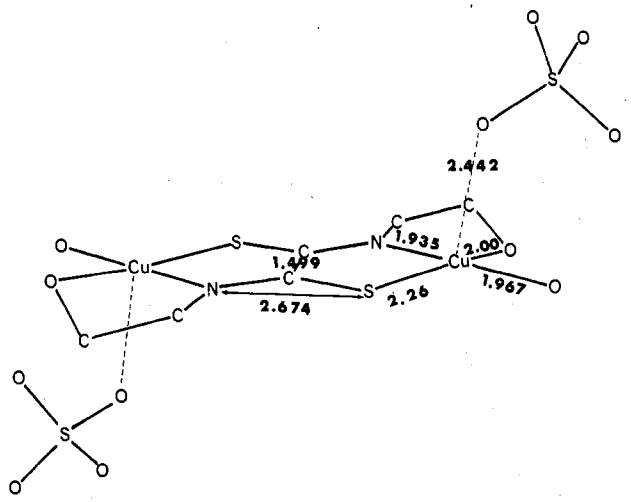

Figure 11. Structure of $Cu_2C_2S_2(NCH_2CH_2OH)_2SO_4 \cdot 2H_2O$.[31]

the $CuC_2O_4 \cdot {}^1/_3H_2O$ chain and the equality of J for these two compounds is not surprising.

The same comparison may be made between $CuC_2O_4 \cdot {}^1/_3H_2O$ and $Cu_2C_2S_2(NCH_2CH_2OH)_2 \cdot 2H_2O \cdot SO_4$, but here the exchange is reinforced by a strong overlap of the sulfur and nitrogen orbitals (Figure 11).[31]

The comparison between $CuC_2O_4 \cdot {}^1/_3H_2O$ and $Cu_2C_2O_4(Et_5dien)_2(BPh_4)_2$ or $Cu_2C_2O_4(dien)_2(ClO_4)_2$ is also interesting. In this case, the exchange parameter is small but the Cu(II) coordination is also very different in spite of the apparent similarity. It has been shown[25] that in the later compounds the magnetic orbital of the Cu(II) ion is different in orientation. At this stage, it is possible to assume that the σ-exchange pathway between $d_{x^2-y^2}$ orbitals schematized in Figure 10 is essential. When it is lacking, a drastic diminution of $|J|$ results.

An interesting point is the consistency of the upper assumption with the observed value of $|J|$ for different metal oxalates of the same ribbon structure (Table III). Let us use the proposed expression for J_{AF} in a binuclear complex[32]

$$J_{AF} = -\frac{2}{n^2}\sum_{\mu=1}^{n}\Delta_\mu S_{\mu\mu} \qquad (4)$$

where $S_{\mu\mu}$ is the overlap integral between two magnetic orbitals of the same symmetry μ centered on each transition ion, Δ_μ the energy splitting of the molecular orbitals built from these magnetic orbitals, and n the number of unpaired electrons on each ion. If the σ-exchange pathway is actually preponderant, the most important term in eq 3 is $\Delta d_{x^2-y^2}$ and the sum is reduced to a single term.[27,36] Assuming that the overlaps between $d_{x^2-y^2}$ magnetic orbitals are much the same in Cu(II), Ni(II), Co(II), and Fe(II) compounds, $|J|$ varies as $1/n^2$ and the following sequence is expected: $J_{Cu} = -272$ cm^{-1}, $J_{Ni} = -68$ cm^{-1}, $J_{Co} = -30$ cm^{-1}, $J_{Fe} = -17$ cm^{-1}. As shown in Table III, a fair agreement is reached.

Acknowledgment. We are grateful to Dr. R. Fourme and Professor O. Kahn for helpful discussions. We express our thanks to D. Dagneaux, A. Fontaine, P. Lagarde, H. Launois, M. Lemonnier, G. Morel, J. Petiau, and D. Raoux, who either are involved in EXAFS experiments or are in the technical support group at LURE, and to Dr. Marin and his collaborators from the LAL (Laboratoire de l'Accélérateur Linéaire at Orsay), who operated the storage ring DCI.

Registry No. CuC_2O_4, 814-91-5; $Fe(C_2O_4) \cdot 2H_2O$, 55703-34-9; $Cu_2(OH)_2(bpy)_2(NO_3)_2$, 17685-95-9; $Cu_2(CH_3CO_2)_4pyz$, 51798-90-4.

References and Notes

(1) LURE: CNRS laboratory associated with the Université de Paris-Sud.
(2) (a) Laboratoire de Physicochimie Structurale and LURE. Address correspondence to author at LURE. (b) Laboratoire de Spectrochimie des Elêments de Transition. (c) Laboratoire de Chimie Théorique and LURE.
(3) L. Dubicki, C. M. Harris, E. Kokot, and R. L. Martin, *Inorg. Chem.*, **5**, 93 (1966).
(4) B. N. Figgis and D. J. Martin, *Inorg. Chem.*, **5**, 100 (1966).
(5) K. T. McGregor and Z. G. Soos, *Inorg. Chem.*, **15**, 2159 (1976).
(6) R. W. Jotham, *J. Chem. Soc., Chem. Commun.*, 178 (1973).
(7) J. Garaj, H. Langfelderova, G. Lundgren and J. Gazo, *Collect. Czech. Chem. Commun.*, **37**, 3181 (1972).
(8) (a) C. Mazzi and F. Garavelli, *Period. Mineral.*, **26**, No. 2–3 (1957); S. Caric, Bull. *Soc. Fr. Mineral. Cristallogr.*, **82**, 50 (1959). (b) Since completion of this work we have found in the literature a powder diffraction study of $CuC_2O_4 \cdot {}^1/_3H_2O$ which confirms qualitatively our model with substantial differences in bond distances: Schmittler, *Monatsber. Dtsch. Akad. Wiss. Berlin*, **10**, 581 (1968).
(9) C. G. Van Kralingen, J. A. C. Van Ooijen, and J. Reedijk, *Transition Met. Chem.*, **3**, 90 (1978).
(10) J. S. Valentine, A. J. Silverstein, and Z. G. Soos, *J. Am. Chem. Soc.*, **96**, 97 (1974); B. Morosin, R. C. Hughes, and Z. G. Soos, *Acta Crystallogr., Sect. B*, **31**, 762 (1975).
(11) R. B. Shulman, P. Eisenberger, W. E. Blumberg, and N. A. Stombaugh, *Proc. Natl. Acad. Sci. U.S.A.*, **72**, 4003 (1975).
(12) J. Reed, P. Eisenberger, B. K. Theo, and B. M. Kincaid, *J. Am. Chem. Soc.*, **99**, 5217 (1977).
(13) P. Eisenberger and J. Reed, *Acta Crystallogr., Sect. B*, **34**, 344 (1977).
(14) S. P. Cramer, K. O. Hodgson, E. I. Stiefel, and W. E. Newton, *J. Am. Chem. Soc.*, **100**, 2748 (1978).
(15) A. Fontaine, P. Lagarde, D. Raoux, M. P. Fontana, G. Maisano, P. Migliardo, and F. Wanderlingh, *Phys. Rev. Lett.*, **41**, 7, 504 (1978).
(16) A. Fontaine, P. Lagarde, A. Naudon, D. Raoux, and P. Spanjaard, *Rapidly Quenched Met., Int. Conf. 3rd* (1978).
(17) R. G. Shulman, P. Eisenberger, and B. M. Kincaid, *Annu. Rev. Biophys. Bioenerg.*, **7**, 559 (1978).
(18) S. P. Cramer and K. O. Hodgson, submitted for publication in *Adv. Inorg. Chem.*
(19) E. A. Stern, D. E. Sayers, and F. W. Lyttle, *Phys. Rev. B*, **11**, 4836 (1975).
(20) C. A. Ashley and S. Doniach, *Phys. Rev. B*, **11**, 1279 (1975).
(21) P. Lee and G. Beni, *Phys. Rev. B*, **15**, 2862 (1977).
(22) B. K. Teo, P. A. Lee, A. L. Simons, P. E. Eisenberger, and B. M. Kincaid, *J. Am. Chem. Soc.*, **99**, 3854 (1977).
(23) R. J. Majeste and E. A. Meyers, *J. Phys. Chem.*, **74**, 3497 (1970).
(24) Except for the dihydroxo complex which has been reported at S.S.R.P., Stanford University, by J. Goulon and J. Kerby.
(25) T. R. Feltouse, E. J. Laskowski, and D. N. Hendrickson, *Inorg. Chem.*, **16**, 1077 (1977).
(26) V. M. Crawford, M. W. Richardson, J. R. Wasson, D. J. Hodgson, and W. E. Hatfield, *Inorg. Chem.*, **15**, 2107 (1976).
(27) Y. Journaux and O. Kahn, *J. Chem. Soc., Dalton Trans.*, in press.
(28) S. de S. Barros and S. A. Friedberg, *Phys. Rev.*, **141**, 637 (1966).
(29) L. Cavalca, A. Chiesivilla, A. Gaetani Monfredotti, and A. Mangia, *J. Chem. Soc., Dalton Trans.*, 393 (1972).
(30) N. F. Curtis, I. R. N. McCormick, and T. N. Waters, *J. Chem. Soc., Dalton Trans.*, 1537 (1973).
(31) J.-J. Girerd, S. Jeannin, Y. Jeannin, and O. Kahn, *Inorg. Chem.*, **17**, 3034 (1978).
(32) J.-J. Girerd, M. F. Charlot, and O. Kahn, *Mol. Phys.*, **34**, 1063 (1977).
(33) R. Dingle, M. E. Lines, and S. L. Holt, *Phys. Rev.*, **187**, 643 (1969).

(34) G. L. McPherson and J. Rong Chang, *Inorg. Chem.*, **15**, 1018 (1976).
(35) M. F. Charlot, J.-J. Girerd, and O. Kahn, *Phys. Status. Solidi B*, **86**, 497 (1978).
(36) P. J. Hay, J. C. Thibeault, and R. Hoffmann, *J. Am. Chem. Soc.*, **97**, 4884 (1975).
(37) O. Kahn and B. Briat, *Colloq. Int. C.N.R.S.*, No. **255**, 251 (1977).
(38) Since E_0 and the phase shifts are strongly correlated, a starting choice of the energy threshold is effectively arbitrary. E_0 is then affined in the fitting procedure.
(39) Such a coordination site was found in $Na_2Cu(C_2O_4)_2 \cdot 2H_2O$, the structure of which has been solved by A. Gleizes, private communication.
(40) O. Kahn, P. Tola, J. Galy, and H. Coudane, *J. Am. Chem. Soc.*, **100**, 3931 (1978); W. E. Estes, J. R. Wasson, J. W. Hall, and W. E. Hatfield, *Inorg. Chem.*, **17**, 3657 (1978).

Contribution from the Laboratoire de Chimie des Métaux de Transition, Equipe de Recherche Associée au CNRS No. 608, Université Pierre et Marie Curie, 75230 Paris Cedex, France

X-ray Study of $(NH_4)_7[H_2AsW_{18}O_{60}] \cdot 16H_2O$: First Example of a Heteropolyanion Containing Protons and Arsenic(III)

Y. JEANNIN* and J. MARTIN-FRÈRE

Received March 29, 1979

The crystal structure of ammonium 18-tungstoarsenate(III), $(NH_4)_7[H_2AsW_{18}O_{60}] \cdot 16H_2O$, has been determined from three-dimensional X-ray data measured on a computer-controlled four-circle diffractometer at room temperature. The compound crystallizes in the monoclinic space group $C2/c$; lattice constants are $a = 21.937$ (5) Å, $b = 14.239$ (5) Å, $c = 22.177$ (9) Å, $\beta = 96.95$ (2)°, and $Z = 4$. The structure has been refined by a full-matrix least-squares method to a final R factor of 0.066 for 6219 observed reflections. No correction could be applied for absorption. The $[H_2AsW_{18}O_{60}]^{7-}$ heteropolyanion is built up with two XW_9O_{33} units sharing six oxygen atoms and joined in a C_i fashion. Inside the first XW_9O_{33} unit is As(III) with its lone pair directed toward the second unit. As revealed by NMR, this polyanion contains two protons inside, which cannot be titrated; thus the two XW_9O_{33} units are different: one of them contains arsenic(III) and the other two protons.

Introduction

In the last few years, several structures of tungsten or molybdenum heteropolyanions have been solved by X-ray, particularly those belonging to series with general formulas $[XM_{12}O_{40}]^{(8-n)-}$, $[XM_9O_{34}]^{(14-n)-}$, and $[X_2M_{18}O_{62}]^{(16-2n)-}$, where X is the heteroatom, n its oxidation number, and M molybdenum or tungsten.[1-12] In this paper we shall use the shortened schematic notation XM_{12}, XM_9, X_2M_{18}.

All these compounds have structures of the "Keggin type"[13] or closely related to it. The heteroatom is either a fourth column element or a fifth column element with oxidation number 5.

However, heteropolyanions can also be prepared where the heteroelement still belongs to the fifth column but has oxidation number 3. Already published studies carried out in our laboratory showed that such a compound may be particularly highly condensed; for example, $[NaSb_9W_{21}O_{86}]^{18-}$ or $[NaAs_4W_{40}Co_2O_{140}]^{23-}$ can be prepared[14-16] and they are stable in neutral solutions. Working with acid solution (pH $\simeq$3) we previously reported a condensed species of schematic formula AsW_{18} which contains arsenic(III).[17]

The As/W ratio seems surprising with respect to the known structure of polyanions containing 18 tungsten atoms known as the "Dawson structure".[18] It is related to the Keggin structure [13] as follows: three adjacent corner-linked octahedra are removed from the Keggin anion, one from each of three edge-sharing W_3O_{13} groups; it gives a XW_9 unit. Two such units are joined in X_2W_{18} by sharing six oxygen atoms; thus they contain two heteroatoms.

Another interesting aspect of $As^{III}W_{18}$ is that arsenic(III) is not tetracoordinated in oxo compounds while the heteroatom is tetracoordinated in X_2M_{18} polyanions having the Dawson structure.[18]

In order to throw light upon these points, we solved the structure of this compound by X-ray diffraction.

Experimental Section

Crystal Synthesis and Chemical Analysis. A 330-g sample of sodium tungstate and 5.5 g of diarsenic trioxide were added into 350 cm^3 of water and boiled. After dissolution of the mixture, 140 cm^3 of a concentrated hydrochloric acid solution (d 1.19) was added under stirring. The solution was kept boiling for 15 min. Yellow crystals appeared after 15 h. As shown by chemical analysis, the As/W ratio was equal to 1/18 and the cation was sodium.

In order to prepare crystals containing ammonium cations which are more suitable for crystallographic study, we dissolved 130 g of the sodium salt in 150 cm^3 of hot water, and 100 cm^3 of a 13% NH_4Cl aqueous solution was then poured into the solution. Slow evaporation led to yellow crystals which were purified by several recrystallizations from water.

Chemical analysis was carried out as follows: the complex was destroyed by sodium hydroxide; ammonium cations were displaced and ammonia was titrated by acidimetry on a first part; on a second part, arsenic(III) was determined by iodometry after tungsten complexation by phosphate; on a third part, tungsten was precipitated by cinchonin and then ignited and weighed as tungsten trioxide.

Anal. Calcd for $(NH_4)_7[H_2AsW_{18}O_{60}] \cdot 16H_2O$: As, 1.57; W, 69.5; N, 2.06. Found (first sample): As, 1.59, 1.59; W, 69.7, 69.3; N, 1.97, 2.03; Cl, ≤0.2. Found (second sample): As, 1.57, 1.58; W, 69.7, 68.7; N, 2.00, 2.02; Cl, ≤0.2.

From these results it was inferred that the compound contains 18 tungsten atoms and 7 ammonium ions for 1 arsenic atom.

Potentiometric titration with sodium hydroxide showed that this salt has no proton which can be titrated. Charge balance led to the formula $(NH_4)_7AsW_{18}O_{59} \cdot nH_2O$.

We measured the amount of water by thermogravimetric analysis. The number of water molecules was between 16 and 18.

Crystallographic Data. Preliminary Laue and precession photographs showed a monoclinic unit cell.

Systematically absent reflections were $h + k = 2n + 1$ for hkl and $l = 2n + 1$ for $h0l$. This is characteristic of $C2/c$ and Cc.

A crystal shaped approximately as a parallelepiped with approximate dimensions 0.12 × 0.12 × 0.07 mm was set up on a computer-controlled four-circle Philips PW 1100 diffractometer.

Lattice constants, determined by least squares from 25 reflections, are $a = 21.937$ (5) Å, $b = 14.239$ (5) Å, $c = 22.177$ (9) Å, $\beta = 96.95$ (2)°, and $V = 6876$ Å^3.

The density of crystals was measured by pycnometry in cyclohexane. The obtained value of 4.58 g/cm^3 led to 4 molecules per unit cell; the calculated value is then 4.57 if the formula is $(NH_4)_7AsW_{18}O_{59} \cdot 17H_2O$.

A total of 9588 independent reflections were collected at room temperature: radiation Mo Kα; graphite monochromator; scan type θ–2θ; scan speed 0.016° s^{-1}; scan length (0.90 + 0.30 tan θ) degrees, if θ is Bragg angle; background measurements in fixed position before and after every scan during a time equal to half of the scan time; maximum recording angle $\theta_{Bragg} = 30°$; standard reflections $\bar{8}22$, $8\bar{2}2$, and 040 measured every 2 h. No decrease of standards was observed.

0020-1669/79/1318-3010$01.00/0